ACS Photonics

Article

pubs.acs.org/journal/apchd5

Bendable III-N Visible Light-Emitting Diodes beyond Mechanical Flexibility: Theoretical Study on Quantum Efficiency Improvement and Color Tunability by External Strain

Shahab Shervin,[†] Seung-Hwan Kim,[†,§] Mojtaba Asadirad,[†] S. Yu. Karpov,[∥] Daria Zimina,[⊥] and Jae-Hyun Ryou*[,†,‡]

[†]Department of Mechanical Engineering, Materials Science and Engineering Program and [‡]Texas Center for Superconductivity at the University of Houston (TcSUH), University of Houston, Houston, Texas 77204-4006, United States

[§]Metamaterial Electronic Device Research Center, Hongik University, Seoul 121-791, Korea

[∥]STR Group, Inc., Engels Avenue 27, P.O. Box 89, 194156, St.-Petersburg, Russia

[⊥]STR US, Inc., 10404 Patterson Avenue, Suite 108, Richmond, Virginia 23238, United States

ABSTRACT: We show that bending of flexible light-emitting diodes based on polar group III−V nitride structures can function as more than mechanically flexible devices through numerical studies. Controlled external bending can improve internal quantum efficiencies and electron-to-photon conversion efficiencies. Moreover, emission wavelength and color can be changed using active polarization control with external bending strains. We show that applying external strain on InGaN/GaN quantum-well (QW) heterostructures can mitigate or enhance the quantum-confined Stark effect. Significant IQE improvement (≥10%) is estimated by introducing external strain with concave-side up bending of flexible heterostructures. We also show significant wavelength shifts in peak emission. Especially, the $In_{0.35}Ga_{0.65}N$ QW can be tuned in the overall visible spectral range by choosing different curvatures and bending modes. We have suggested the concept of a photoelectromechanical device that can emit different colors depending on the applied external strain varying from red to blue, enabling white light generation with the same active region consisting of QWs with a constant indium mole fraction.

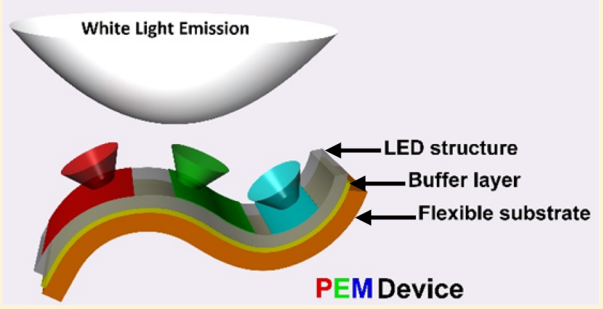

KEYWORDS: *strain, light-emitting diodes, quantum-confined Stark effect, polarization, quantum efficiency, wavelength tunability*

Recent developments in flexible electronics demonstrate that semiconductor materials can be very flexible when their thickness is small enough (on the order of micrometers or less), deviating from the brittle nature of bulk properties.[1,2] In an effort of the development of flexible display applications, flexible visible light-emitting diodes (LEDs) have been developed.[3−9] When the semiconductor structure becomes flexible on a flexible template/substrate, it can be used in many applications of wearable and implantable electronics,[10,11] and most previous studies have focused on such aspects of flexible LEDs, while fewer explored the contribution of external strain on the device performance. Recently, we have investigated the effects of applying external strain on the performance of flexible transistors.[12] In the present study, we suggest that the flexible LEDs based on group III−V nitride (III-N) materials, which is the most important material in solid-state lighting for energy savings, can be more than just a mechanically flexible device. They can be equipped with new functionalities and improved quantum efficiencies (QEs) by taking advantage of the flexibility.

III-N materials and devices have brought tremendous benefits to mankind as energy-efficient and environmentally friendly light sources.[13] The potential of the materials has been recognized in many applications of current- and next-generation electronics and photonics.[14,15] Unlike other semiconductors including silicon (Si) and gallium arsenide (GaAs), of which device structures are constructed on the same type of single-crystalline substrates, native single-crystalline substrates of gallium nitride (GaN) were not available until very recently.[16] Development of "device-quality" GaN and related materials had been hampered for about 17 years,[17] since the first attempt of the epitaxial growth of GaN,[17,18] until Amano and Akasaki developed a special epitaxial growth technique using a low-temperature buffer layer.[19] This strained hetero-epitaxial growth works well only for the growth along the *c*-direction, that is, to yield a (0001) plane surface of wurtzite structure of GaN. Hence, most III-N materials are grown epitaxially in a polar direction with a group-III-element-terminated surface such as a gallium (Ga) face. Such a direction of wurtzite materials contains both macroscopic spontaneous and piezoelectric polarizations.[20] Whereas the

Received: December 24, 2015
Published: February 8, 2016

DOI: 10.1021/acsphotonics.5b00745
ACS Photonics 2016, 3, 486−493

effects of polarizations do not prevent the materials from functioning as working devices, they pose challenges to enhance quantum efficiencies in the photon generation of light-emitting devices.[21]

Limited quantum efficiencies are associated with a quantum-confined Stark effect (QCSE).[22] The QCSE is intrinsic to III-N quantum-well (QW) structures grown on a (0001) plane without applying a bias. In III-N QW heterostructures, the polarizations induce charges at the interfaces and result in gradients for electronic band structures of the layers in equilibrium. $In_xGa_{1-x}N$/GaN multiple QWs (MQWs), which are commonly used in an active photon generation region of visible LEDs, laser diodes (LDs), and white solid-state lighting lamps, are also affected by the QCSE.[23] It is related to lower radiative recombination rates[24,25] and also possibly one of the origins of efficiency droop in visible LEDs.[26] Tilted conduction and valence bands of the QW lead to a spatial separation of electron and hole wave functions and a red shift in peak emission wavelength due to a narrower effective band gap. To increase the probability of radiative recombination, the overlap of electron and hole wave functions should be enhanced. In fact, the QWs in III-N heterostructures have generally thinner layers (2−3 nm each) than those in other III−V heterostructures, e.g., QWs of GaAs- and InP-based heterostructures (∼>5 nm each), to partially improve the overlap.

Different strategies have been suggested to mitigate the QCSE. First, epitaxial structures were grown in nonpolar and semipolar directions,[27] for example, the QWs on a (11−20) *a*-plane and a (10−10) *m*-plane,[28,29] and those on semipolar planes[30] to reduce the magnitude of the polarization-induced electric field in the growth direction across the QWs.[31] However, the epitaxial growth in nonpolar and semipolar directions has been marginally successful only on native substrates,[32,33] which may not be easily implemented in low-cost and general-lighting applications. The second method is to modify epitaxial layer structures including changes in the lattice constants of layers below and above the QWs.[34,35] The control of polarizations has been focused mainly on the effects from differential spontaneous polarization and lattice strain that are set by the layers of epitaxial structures. For both strategies, the degree of freedom in controlling the polarizations is very limited, which requires modifications in epitaxial structures or substrate orientations. In this work, we study the polarization effects and related fundamental electronic band structure changes beyond the limit of lattice strain for active and high-degree control of polarizations by applying external strain.

To apply external strain, the structure should be able to deform in response to external loading conditions. Applying external strain on the III-N structures grown on nonflexible single-crystal substrates is nearly impossible due to the brittle nature of the substrates. When epitaxial structures become thin films and free from rigid substrates, the semiconductor epitaxial structures on flexible substrates can withstand a high degree of strain.[1,2] In this numerical study, we show that externally controlled bending strain on flexible III-N structures can enhance internal quantum efficiencies (IQEs) and electron-to-photon conversion efficiencies. Moreover, we suggest the concept of a photoelectromechanical device (PEM), which can emit different colors of light based on different amounts of applied external strain. According to the concept, one can use external strain to emit blue and red color from flexible green LEDs, which can be ultimately used for white light generation.

METHODS

Computational simulation was performed using the SiLENSe 5.8 package (STR)[36] which is intended for modeling the operation of LED and laser diode heterostructures based on direct-band-gap wurtzite semiconductors of group III-N and group II oxides. The software simulates the band diagrams as a function of bias, electron, and hole transport inside a heterostructure, nonradiative and radiative carrier recombinations that provide light emission. The optical module employs Schrödinger equations for electrons and holes with the potential energy determined from a self-consistent solution of the Poisson and drift-diffusion transport equations. While many technology computer-aided design (TCAD) device simulators for photonic and electronic devices are available, they cannot be used in the calculation of flexible devices with active external loading. This package was modified to simulate the effects of applying external strain on the different characteristics of III-N LEDs. Whereas applying uniaxial or biaxial strain (stretching) on conformal III-N thin-film heterostructures is straightforward in computation, it is challenging experimentally by external load. Therefore, we focus on the external load by bending to apply strain in the numerical study.

Figure 1 shows a schematic cross-section and bending conditions of a flexible III-N light-emitting heterostructure used

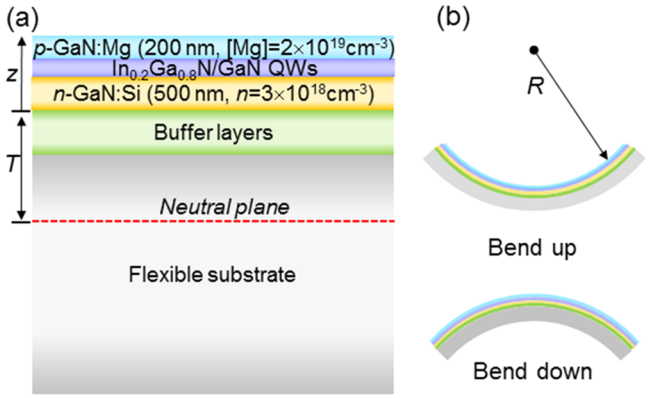

Figure 1. (a) Schematic cross-section for layers of flexible visible light-emitting diodes (LEDs) and (b) bending conditions for bend-up and bend-down. The LED heterostructure consists of an active region of InGaN quantum wells (QWs) with GaN QW barriers (QWBs) imbedded in a p−n junction (p-GaN/n-GaN) on a flexible substrate. Bending the flexible structure with its concave side up and down are defined as "bend-up" and "bend-down" conditions, respectively.

in this study. The whole structure consists of a flexible substrate and III-N layers. The dotted line is a neutral plane where no net strain is applied during bending. A position of the neutral plane in a hybrid structure, $Z(\varepsilon = 0)$, is estimated by

$$Z(\varepsilon = 0) = \frac{\sum_{i=1}^{n} E_i d_i \left[\left(\sum_{j=1}^{i} d_j \right) - \frac{d_i}{2} \right]}{\sum_{i=1}^{n} E_i d_i} \quad (1)$$

where E_i and d_i are the elastic modulus and thickness of the ith layer, respectively. Equation 1 assumes linear mechanics, pure bending, and no-slip boundaries between the layers. These assumptions are valid in the case of moderate bending (bending radius, $R \gg \sum_{i=1}^{n} d_i$).[37] Young's modulus of III-N layers is ∼260 GPa.[38] For various flexible substrates, the values of moduli are ∼0.3−0.8, ∼ 200, and ∼220 GPa for polydime-

DOI: 10.1021/acsphotonics.5b00745
ACS Photonics 2016, 3, 486−493

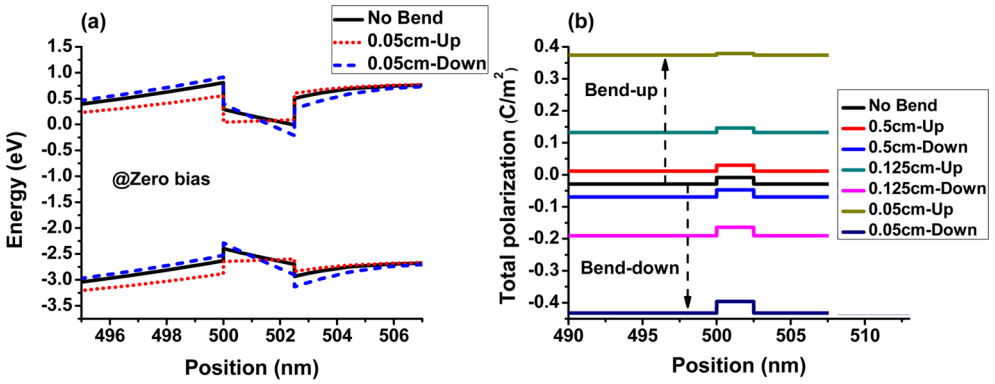

Figure 2. (a) Equilibrium electronic band diagrams and (b) total polarization changes of a single-quantum-well (SWQ) structure with different radii of curvature, *R*. Applying external strain by bending the LED device changes the band structure and induced total polarization in QWs.

thylsiloxane, Hastelloy,[39] and yttria-stabilized zirconia films,[40] respectively.[41,42] If a different material is used for the substrate, the neutral plane position is changed accordingly. When the Young's moduli of the thin-film layer (III-N material) and the flexible substrate are similar, the neutral plane is usually located in the substrate, which is significantly thicker. In this case, the III-N layers experience only one type of strain, either in-plane compressive or in-plane tensile. Figure 1 also defines bending conditions. Bending with the structure's concave side up is defined as a "bend-up" condition, resulting in compressive strain in III-N layers. Bending down with the structure's concave side down (convex side up), that is, "bend-down", will induce tensile strain in the III-N layers. Unlike the uniaxial and biaxial strains, the lattice mismatch by bending is not constant in a layer of the epitaxial structures. The position-dependent in-plane lattice mismatch, η_a, is calculated by

$$\eta_a = \frac{(a_B - a_L)}{a_B} + \frac{Z + T}{R} \tag{2}$$

where a_B and a_L are bulk in-plane lattice parameters of the buffer (GaN in this study) and layer (before epitaxial growth, InGaN or GaN in this study); T is the distance between the neutral plane and the first layer of III-N heterostructures (*n*-GaN in this case); Z is a position variable in a vertical coordinate from the bottom of the first layer; and R is a radius of curvature. It is assumed that the grown epitaxial layers are pseudomorphic. The sign of R is designated negative and positive for the bend-up and bend-down conditions, respectively. The first and second terms in eq 2 are related to the strains from built-in lattice mismatch and external strain by bending, respectively. We used a value of 200 μm for T in this study, and R was varied to investigate the effect of bending degree. The radius of curvature, R, was changed from −0.05 cm (−0.05, −0.125, −0.25, −0.5, −1 cm, bend-up) to ∞ (no-bend) and then to 0.05 cm (1, 0.5, 0.25, 0.125, 0.05 cm, bend-down). The curvature was changed from −20 cm^{-1} for bend-up conditions to 20 cm^{-1} for bend-down conditions. The curvatures used in this study appear to be higher than the normal range of flexible electronics; however, the semiconductor structure can withstand a high degree of deformation.[43−46]

The III-N heterostructures consist of InGaN QWs with GaN QW barriers (QWBs) imbedded in a p−n junction, to be compared to actual photon emission devices by carrier injection. The InGaN/GaN QW structure can be a single QW (SQW) or multiple QWs (MQWs). The heterostructure with a SQW consists of a 500 nm thick n-type GaN layer with a doping concentration of $N_D = 3 \times 10^{18}$ cm^{-3} by shallow donor Si (n-GaN:Si, 500 nm, n ≈ [Si] = 3×10^{18} cm^{-3}), an $In_{0.2}Ga_{0.8}N$ QW (2.5 nm), and a p-GaN (200 nm, p < [Mg] = 2×10^{19} cm^{-3}) layer. The InGaN QW with 20% mole fraction of InN was selected to study a typical active region material used in solid-state-lighting white lamps. Free-hole concentration, p, is significantly lower than acceptor doping concentration, N_A = [Mg], due to the deep-level nature of the Mg acceptor in GaN with an activation energy of 170−190 meV.[47] The electron and hole mobilities were assumed to be 100 and 10 cm^2·V^{-1}·s^{-1}, respectively.[48] The heterostructure with MQWs consists of five-period $In_{0.2}Ga_{0.8}N$ QWs (3 nm each) and four GaN QWBs (12 nm each) sandwiched between the same n-GaN and p-GaN layers. The SQW structure is used mainly to study fundamental aspects of the QCSE. The results from the SQW structure are expanded to the MQW structure for further investigation with actual light-emitting device implications.

RESULTS AND DISCUSSION

To investigate the QCSE changes by the effect of external bending strain, a SQW structure is studied. In many device applications, the effects of polarization in QWs have been considered mainly from the contribution of differential spontaneous polarization between an InGaN QW and a GaN QWB and piezoelectric polarization in an InGaN QW. This consideration makes sense for III-N structures epitaxially grown on nonflexible substrates with a GaN buffer layer, as the GaN QWBs are not strained in pseudomorphic III-N layers on the GaN buffer layer. Total polarization of the QW, P_{QW}, by internal lattice strain is calculated as[21]

$$P_{QW} = P_{sp,QW} - P_{sp,QWB} + P_{pz,QW}(\epsilon) \tag{3}$$

where $P_{sp,QW}$ and $P_{sp,QWB}$ are spontaneous polarization fields of QW and QWB, respectively; $P_{pz,QW}(\epsilon)$ is a piezoelectric polarization field of QW; and ϵ is a strain in QW from lattice mismatch. When the external strain is applied, total polarization of the QW, $P_{ex,QW}$, is

$$P_{ex,QW} = P_{sp,QW} - P_{sp,QWB} + P_{pz,QW}(\epsilon_1) - P_{pz,QWB}(\epsilon_2) \tag{4a}$$

$$P_{ex,QW} = P_{total,QW} - P_{total,QWB} = \Delta P_{total} \tag{4b}$$

where $P_{pz,QWB}$ is a piezoelectric polarization field of QWB, and ϵ_1 and ϵ_2 are strains from combinations of lattice mismatch and external strain in QW and QWB, respectively. Bending of the

DOI: 10.1021/acsphotonics.5b00745
ACS Photonics 2016, 3, 486−493

structure leads to a spatial variation of the polarization even in layers of constant composition, as the effective mismatch η_a becomes dependent on the position z according to eq 2. Therefore, a polarization charge proportional to the gradient of the polarization is induced similarly to so-called polarization doping in graded-composition III-N layers.[49,50]

Figure 2a compares equilibrium electronic band diagrams of a SQW region with various bending conditions at zero bias. Band tilt[51] by built-in potential from charges at interfaces of the QW is shown in a no-bend condition, as a result of intrinsic QCSE. External bending strain changes the QCSE. Conduction and valence bands become more flattened and more tilted for bend-up and bend-down conditions, respectively. The total polarization difference between GaN and InGaN in eq 4 is critical to address the induced band tilt and consequent QCSE, as shown in Figure 2b. Especially for the bend-up conditions, while total polarization of each layer increases by compressive strain, the total polarization difference between the QW and QWB decreases. In a bend-up condition of $R = -0.05$ cm, ΔP_{total} is reduced to 0.004 68 C/m^2 from 0.0202 C/m^2 (no-bend). The total polarization difference increases with increasing bend-down condition. ΔP_{total} is 0.0358 C/m^2 at $R = 0.05$ cm. As a result, the QCSE becomes more significant. When charged carriers are injected, spatial distribution of electrons and holes and effective band-gap energies are dependent on band tilt in the QW.

Figure 3 shows wave functions of electrons and holes in the SQW with representative bending conditions at a current

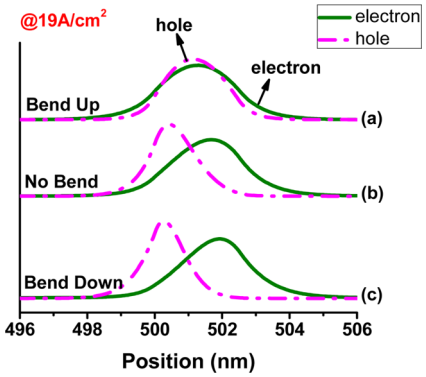

Figure 3. Electron and hole wave functions in a SQW structure after carrier injection in different bending conditions: (a) bend-up with $R = -0.05$ cm, (b) no-bend, and (c) bend-down with $R = 0.05$ cm. The effect of bending mode can be seen, whereas in bend-up mode electron and hole wave function almost overlap completely, while for bend-down mode the spatial distance between the election and hole wave function increases compared to the no-bend mode.

density of $J \approx 19$ A/cm^2 in the p−n junction diode. In the bend-up condition, the wave functions of electrons and holes move closer to be more overlapped. In contrast, they are separated farther with increasing bend-down condition from a no-bend condition. The degree of separation in electron and hole wave functions affects the oscillator strength of carriers and, hence, the radiative recombination probability (rate). Radiative recombination rates competing against nonradiative recombination rates, including Shockley−Read−Hall and Auger recombinations, determines IQE (η_{int}) of photon emitters, defined by

$$\eta_{int} = \frac{R_r}{R_r + R_{nr}} \tag{5}$$

where R_r is a radiative recombination rate and R_{nr} is a nonradiative recombination rate. The modification in QCSE changes dominant transition energies.

Figure 4 shows changes in IQE and peak emission wavelength of a SQW structure as a function of curvature. By applying external strain with bend-up, the IQE improves with increasing curvature from the no-bend condition. On the other hand, bending-down of an SQW structure makes the IQE lower with more strain. The QCSE is also affected by the density of the injected carrier. Figure 4a and b compare IQE and peak emission wavelength changes in low ($J \approx 19$ A/cm^2) and high ($J \approx 500$ A/cm^2) injection conditions, respectively. At low current density (Figure 4a), bending-up results in increases in the IQE by ∼11% from 67% (no bend) to 78% (bend-up with $R = -0.05$ cm). Also, mitigated QCSE by external strain makes an effective band gap wider. When the bending condition changes from no-bend to bend-up conditions at $R = -0.05$ cm, the emission peak from the QW shifts toward shorter wavelength (blue shift) by $\Delta\lambda_{blue} \approx 10$ nm. On the other hand, bending-down degrades the IQE by ∼6% from 67% (no-bend) to 61% (bend-down with $R = 0.05$ cm), and the red shift (peak wavelength toward longer wavelength) is $\Delta\lambda_{red} \approx 18$ nm. Under high injection, the IQE and peak wavelength changes are moderate compared to those under low injection. Figure 4b shows the IQE improvement by ∼4% and $\Delta\lambda_{blue} \approx 9$ nm by bending up. The IQE decreases by ∼7% and $\Delta\lambda_{red} \approx 13$ nm by bending down. In high injection conditions, the QCSE is partially screened by free carriers;[52] therefore, improvement or degradation of IQE and peak emission wavelength shift by bending becomes less significant.

The five-period MQW structure is similar to the active region of conventional III-N-based LEDs. Figure 5a shows current−voltage (I−V) characteristic of a p−n junction diode with MQWs with different radii of curvature. Tht turn-on voltage decreases by bending up, while it increases by bending down. Figure 5b shows band structures at 3-V bias for bend-down and bend-up ($R = \pm 0.05$ cm) and no-bend conditions. The barriers for the transport of electrons and holes increase in bend-down conditions compared to a no-bend condition, and they decrease in bend-up conditions. As a result, the threshold voltage for the maximum bend-down condition is highest among all the bending conditions. In a bend-up condition with $R = -0.05$ cm, the I−V curve shows a rapid turn-on. This diode electrical characteristic suggests that electrical−photon power conversion efficiencies (wall-plug efficiencies) should be even higher than the already enhanced IQEs for the case of LEDs with bend-up conditions. Figure 5b also shows mitigation or enhancement of the QCSE depending on the bending conditions similar to the cases of SQWs.

Figure 6a and b compare IQE and peak emission wavelength changes in low ($J \approx 20$ A/cm^2) and high ($J \approx 500$ A/cm^2) injection conditions, respectively, with different bending conditions. At low current density (Figure 6a), the IQE in the no-bend condition is 73%, and it increases to 79% (∼6% improvement) for bending up with $R = -0.05$ cm. On the other hand, by bending down, the IQE decreases to 58% by 15% at $R = 0.05$ cm. The peak wavelength changes as a function of curvature with different bending conditions are estimated in Figure 6a. The wavelength shifts are $\Delta\lambda_{blue} \approx 17$ nm and $\Delta\lambda_{red} \approx 18$ nm with $R = -0.05$ and 0.05 cm, respectively. At high

DOI: 10.1021/acsphotonics.5b00745
ACS Photonics 2016, 3, 486−493

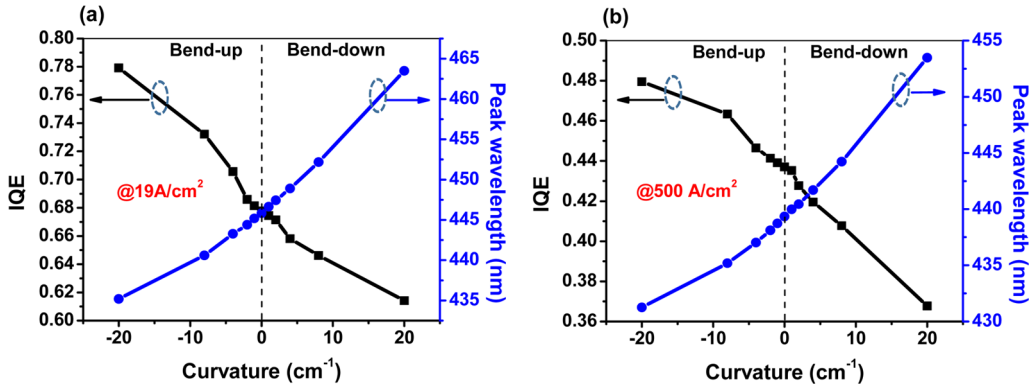

Figure 4. Internal quantum efficiency (IQE) and peak emission wavelength changes of an SQW structure as a function of curvature: (a) low current ($J \approx 19$ A/cm^2) and (b) high current ($J \approx 500$ A/cm^2) injections. For both low and high current injection density, IQE increases by changing the mode of bending from bend-down to no-bend and bend-up eventually. Peak wavelength emissions for low and high current density also show a similar trend. Changing the bending mode from no-bend to bend-down causes a red shift in peak wavelength emission, while in bend-up mode a blue shift occurs.

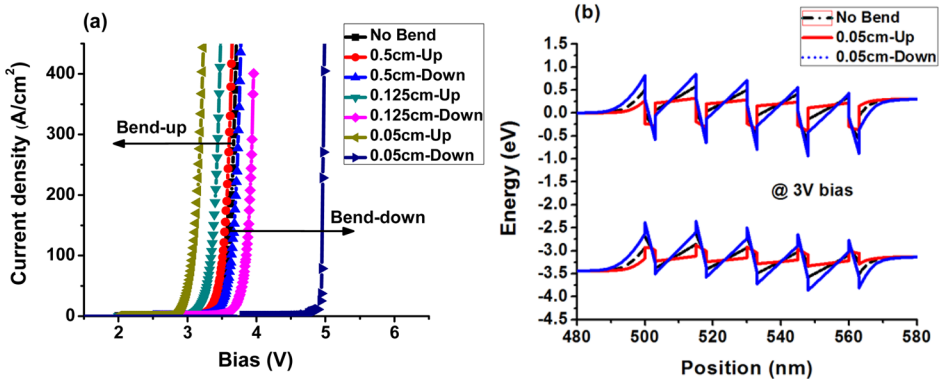

Figure 5. (a) Current−voltage (I−V) curves of a p−n junction diode with multiple quantum wells (MQWs) for different R and (b) energy band diagrams in different bending conditions: bend-up with $R = -0.05$ cm, no-bend, and bend-down with $R = 0.05$ cm. In bend-up mode, by increasing curvature the turn-on voltage decrease, while in the bend-down mode, the LED turns on at higher voltage compared to bend-up and no-bend modes. Comparing the band diagram of the MQW LED for different bending modes shows more tilting for the bend-down mode while more flattening for bend-up mode.

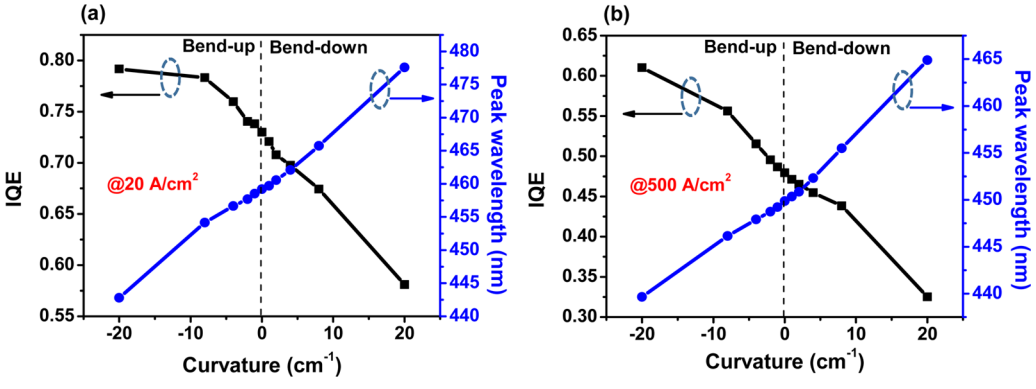

Figure 6. IQE and peak emission wavelength changes of an MQW structure as a function of curvature: (a) low current density ($J \approx 20$ A/cm^2) and (b) high current density ($J \approx 500$ A/cm^2) injections. Similar to the SQW structure, both low and high current injection densities show IQE improvement by changing the mode from bend-down to no-bend and eventually to bend-up mode. Peak wavelength emission shows a blue shift for the bend-up mode, while a red shift occurs for the bend-down mode.

current density (Figure 6b), the IQE also improves by bending up the structure, whereas it decreases in bend-down conditions. The IQE is 48% without bending, and it increases to 61% in a bend-up condition with $R = -0.05$ cm, showing ∼13% improvement. On the other hand, IQE decreases with increasing bending down. The overall IQE values at high current densities are lower than those at low current densities due to spillover effect of carriers (mostly electrons) out of the MQW active region.[53]

Figure 7a shows the total polarization difference between GaN QWBs and InGaN QWs. ΔP_{total} for no-bend, bend-up ($R = -0.05$ cm), and bend-down ($R = 0.05$ cm) conditions are

DOI: 10.1021/acsphotonics.5b00745
ACS Photonics 2016, 3, 486−493

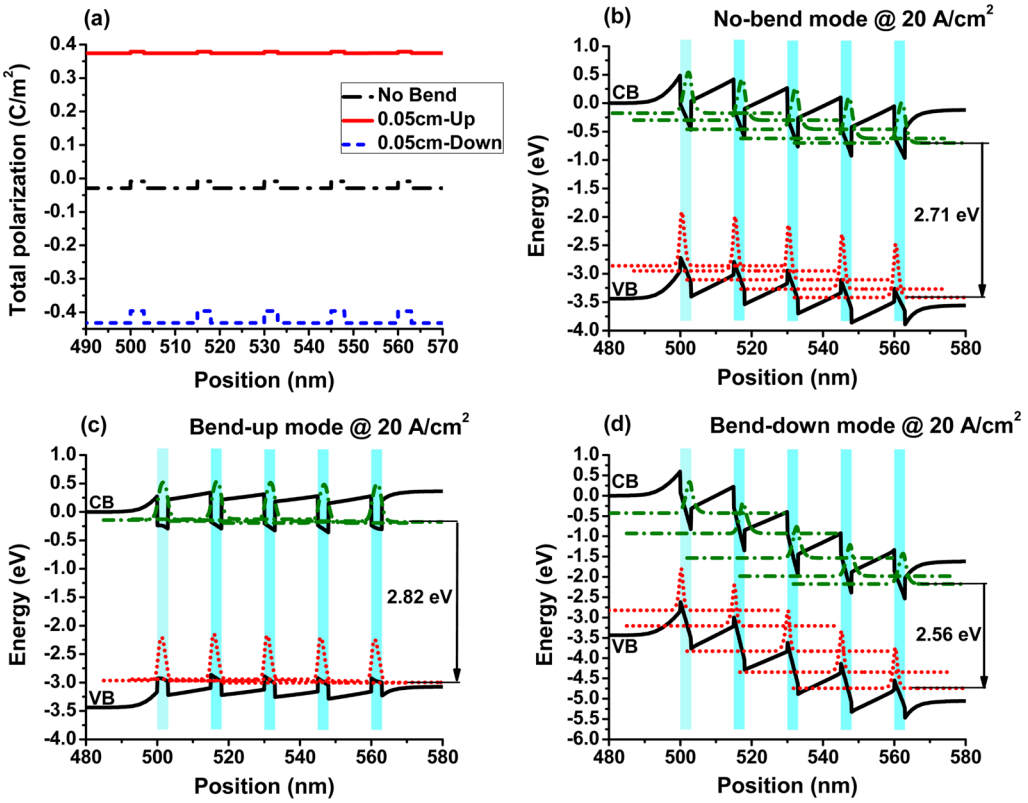

Figure 7. (a) Total polarization changes in three bending conditions: bend-up (solid line), no-bend (dashed dotted line), and bend-down (dotted line); (b–d) energy band diagrams at a current density of $J \approx 20$ A/cm^2 for no-bend, bend-up, and bend-down conditions, respectively, of an MQW structure. Electron wave function is shown by the dashed-dotted curve, and the hole wave function is the dotted curve. Conduction band (CB) and valence band (VB) are defined in the diagrams. The effect of the bending mode and magnitude of curvature on polarization changes are shown. It can be seen through the highlighted area (with blue color) in the quantum wells that the electron and hole overlap increases for the bend-up mode. For the bend-down mode the electron and hole wave functions separate more compared to the no-bend mode.

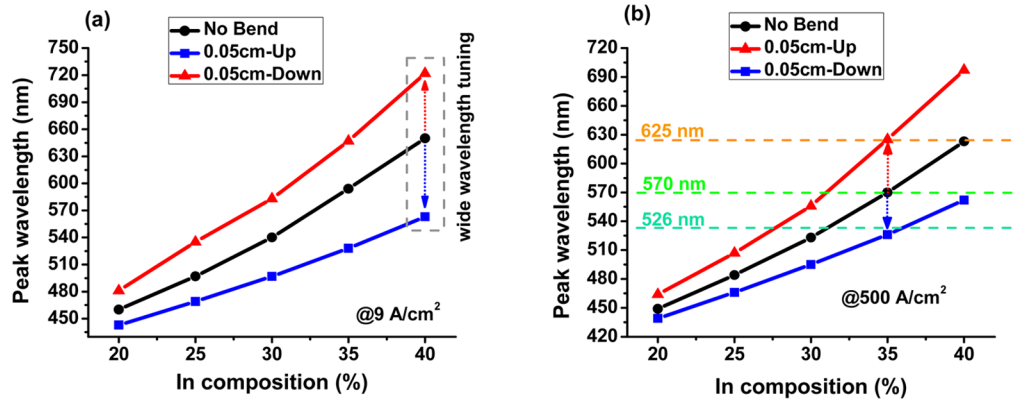

Figure 8. Peak emission wavelength changes as a function of In mole fraction of $In_xGa_{1-x}N$ QWs in a five-period MQW structure in three bending conditions (no-bend, bend-up, and bend-down): peak wavelength changes in (a) low current density ($J \approx 10$ A/cm^2) and (b) high current density ($J \approx 500$ A/cm^2) injections. The concept of peak wavelength emission tunability by changing the bending modes is shown. By choosing the appropriate In mole fraction, in the visible range, it is possible to generate blue and red light by bending up and down the flexible LED structure, respectively, while in the no-bend mode green light is emitting, which eventually results in white light emission without using phosphorus, which is the case for conventional white light LEDs.

0.0202, 0.00468, and 0.0358 C/m^2, respectively. Figure 7b–d compare electronic band diagrams of an MQW region with various bending conditions at a constant current density ($J \approx 20$ A/cm^2). In addition, wave functions of electrons and holes in the MQW are illustrated with representative bending conditions. In the bend-up condition, the spatial separation between wave functions of electrons and holes decreases, and they move closer to be more overlapped. Significant mitigation of the QCSE results in an IQE improvement. Effective band-gap energies of MQWs change depending on the bending conditions, showing 2.71, 2.82, and 2.56 eV for no-bend, bend-up, and bend-down conditions, respectively. The band-gap energies correspond to the emission wavelengths of 456, 440, and 484 nm, respectively. This wavelength tunability can be used in multichannel optical communications for smart lighting applications.[54]

DOI: 10.1021/acsphotonics.5b00745
ACS Photonics 2016, 3, 486–493

Study on the effect of indium (In) mole fraction (x_{In}) (or mole fraction of InN) in $In_xGa_{1-x}N$ QWs is necessary to address additional functionality of flexible LED structures for future applications. Figure 8a and b compare peak emission wavelength changes as a function of x_{In} in MQWs for low ($J \approx 9$ A/cm^2) and high ($J \approx 500$ A/cm^2) current injections. At a low current density ($J \approx 9$ A/cm^2), increasing the In mole fraction results in higher wavelength shifts than high current density ($J \approx 500$ A/cm^2). Various In mole fractions, such as x_{In} = 0.2, 0.25, 0.3, 0.35, and 0.4, were studied. Three bending conditions, namely, no-bend, bend-up ($R = -0.05$ cm), and bend-down ($R = 0.05$ cm), were selected to investigate the external strain effect on the peak wavelength emission shifts. By increasing the In mole fraction (from x_{In} = 0.2 to 0.4), the effect of bending on the peak emission wavelength changes becomes more significant. Blue and red shifts of the peaks by bending become more significant with increasing In mole fraction. At a low current density ($J \approx 9$ A/cm^2), shown in Figure 8a for x_{In} = 0.4, huge shifts are estimated with $\Delta\lambda_{blue}$ = 87 nm and $\Delta\lambda_{red}$ = 72 nm for bend-up and bend-down conditions from the no-bend condition, respectively. By bending the flexible $In_{0.4}Ga_{0.6}N$/GaN MQW LED structure, the tunable peak emission wavelength range is $\Delta\lambda_{total} \approx 160$ nm. Bending the flexible LED structure at high current injection ($J \approx 500$ A/cm^2) provides a unique feature for the flexible $In_xGa_{1-x}N$/GaN MQW LED depending on the In mole fraction. As shown in Figure 8b, at x_{In} = 0.35, it is possible to tune the emitting photon wavelength in the visible range from a green color ($\lambda \approx 570$ nm) for the no-bend mode toward a blue color ($\lambda \approx 526$ nm) by bending up or toward the red color ($\lambda \approx 625$ nm) by bending down. In other words, it is possible to emit a combination of different color elements of visible light covering red (R), green (G), and blue (B) light by bending the flexible $In_xGa_{1-x}N$/GaN MQW LED having the same active region with different radii of curvatures in different bending modes, that is, by forming a corrugated structure of flexible LEDs. This property may enable the realization of white light without changing In mole fraction. Therefore, generation of white light lamps is possible from a flexible InGaN/GaN LED without resorting to phosphor conversion in combination with blue LEDs and combination of individual RGB LEDs having different active region materials.

In summary, we have studied the effects of external bending strain on the quantum-confined Stark effect of quantum wells in wurtzite InGaN/GaN heterostructures on flexible substrates. Our results showed that internal quantum efficiency improves significantly by applying external compressive strain in QW and QWB with bending-up. On the other hand, IQE decreases in bend-down modes due to enhanced QCSE in the QW. We found significant blue shift and red shift in bend-up and bend-down conditions, respectively, compared to the no-bend condition. In addition, we studied the effect of indium mole fraction (x_{In}) in the flexible $In_xGa_{1-x}N$/GaN MQW LEDs. Our results showed that significant tunability in peak emission wavelength is achievable by controlling x_{In}. The blue and red shift of the emission peaks achieved for flexible LEDs can produce red, green, and blue colors. This finding leads us to suggest a concept of a photoelectromechanical device in which peak wavelength emission tuning enables white light emission at a constant In mole fraction by bending the flexible LED structure.

AUTHOR INFORMATION

Corresponding Author

*E-mail: jryou@uh.edu.

Notes

The authors declare no competing financial interest.

ACKNOWLEDGMENTS

J.-H.R. acknowledges partial financial support from Texas Center for Superconductivity at the University of Houston (TcSUH). S.H.K. acknowledges financial support from Basic Science Research Program through the National Research Foundation of Korea (NRF) funded by the Ministry of Education (No. 2015R1A6A1A03031833). The authors acknowledge useful technical discussions with Drs. Kirill Bulashevich and Alex Galyukov of the STR Group.

REFERENCES

(1) Schmidt, O. G.; Eberl, K. Thin Solid Films Roll up into Nanotubes. *Nature* **2001**, *410*, 168−168.

(2) Shahrjerdi, D.; Bedell, S. W. Extremely Flexible Nanoscale Ultrathin Body Silicon Integrated Circuits on Plastic. *Nano Lett.* **2013**, *13*, 315−320.

(3) Kim, R.-H.; Kim, D.-H.; Xiao, J.; Kim, B. H.; Park, S.-I.; Panilaitis, B.; Ghaffari, R.; Yao, J.; Li, M.; Liu, Z.; Malyarchuk, V.; Kim, D. G.; Le, A.-P.; Nuzzo, R. G.; Kaplan, D. L.; Omenetto, F. G.; Huang, Y.; Kang, Z.; Rogers, J. A. Waterproof AlInGaP Optoelectronics on Stretchable Substrates with Applications in Biomedicine and Robotics. *Nat. Mater.* **2010**, *9*, 929−937.

(4) Yoon, J.; Jo, S.; Chun, I. S.; Jung, I.; Kim, H.-S.; Meitl, M.; Menard, E.; Li, X.; Coleman, J. J.; Paik, U.; Rogers, J. A. GaAs Photovoltaics and Optoelectronics using Releasable Multilayer Epitaxial Assemblies. *Nature* **2010**, *465*, 329−333.

(5) Kim, H.-S.; Brueckner, E.; Song, J.; Li, Y.; Kim, S.; Lu, C.; Sulkin, J.; Choquette, K.; Huang, Y.; Nuzzo, R. G.; Rogers, J. A. Unusual Strategies for using Indium Gallium Nitride Grown on Silicon (111) for Solid-State Lighting. *Proc. Natl. Acad. Sci. U. S. A.* **2011**, *108*, 10072−10077.

(6) Jung, Y.; Wang, X.; Kim, J.; Kim, S. H.; Ren, F.; Pearton, S. J.; Kim, J. GaN-Based Light-Emitting Diodes on Origami Substrates. *Appl. Phys. Lett.* **2012**, *100*, 231113.

(7) Sher, C.-W.; Chen, K.-J.; Lin, C.-C.; Han, H.-V.; Lin, H.-Y.; Tu, Z.-Y.; Tu, H.-H.; Honjo, K.; Jiang, H.-Y.; Ou, S.-L.; Horng, R.-H.; Li, X.; Fu, C.-C.; Kuo, H.-C. Large-Area, Uniform White Light LED Source on a Flexible Substrate. *Opt. Express* **2015**, *23*, A1167−A1178.

(8) Lee, S. Y.; Park, K.-I.; Huh, C.; Koo, M.; Yoo, H. G.; Kim, S.; Ah, C. S.; Sung, G. Y.; Lee, K. J. Water-Resistant Flexible GaN LED on a Liquid Crystal Polymer Substrate for Implantable Biomedical Applications. *Nano Energy* **2012**, *1*, 145−151.

(9) Russo, A.; Ahn, B. Y.; Adams, J. J.; Duoss, E. B.; Bernhard, J. T.; Lewis, J. A. Pen-on-Paper Flexible Electronics. *Adv. Mater.* **2011**, *23*, 3426−3430.

(10) Ko, H.; Kapadia, R.; Takei, K.; Takahashi, T.; Zhang, X.; Javey, A. Multifunctional, Flexible Electronic Systems Based on Engineered Nanostructured Materials. *Nanotechnology* **2012**, *23*, 344001.

(11) Park, S. I.; Le, A. P.; Wu, J.; Huang, Y.; Li, X.; Rogers, J. A. Light Emission Characteristics and Mechanics of Foldable Inorganic Light-Emitting Diodes. *Adv. Mater.* **2010**, *22*, 3062−3066.

(12) Shervin, S.; Kim, S.-H.; Asadirad, M.; Ravipati, S.; Lee, K.-H.; Bulashevich, K.; Ryou, J.-H. Strain-Effect Transistors: Theoretical Study on the Effects of External Strain on III-Nitride High-Electron-Mobility Transistors on Flexible Substrates. *Appl. Phys. Lett.* **2015**, *107*, 193504.

(13) The Nobel Prize in Physics 2014. http://www.nobelprize.org/nobel_prizes/physics/laureates/2014/press.html.

(14) Nakamura, S. The Roles of Structural Imperfections in InGaN-Based Blue Light-Emitting Diodes and Laser Diodes. *Science* **1998**, *281*, 956−961.

DOI: 10.1021/acsphotonics.5b00745
ACS Photonics 2016, 3, 486−493

(15) Pearton, S. J.; Ren, F. GaN Electronics. *Adv. Mater.* **2000**, *12*, 1571−1580.
(16) Ryou, J.-H. Gallium Nitride (GaN) on Sapphire Substrates for Visible LEDs. In *Nitride Semiconductor LEDs: Materials, Performance and Application*; Huang, J.-J.; Kuo, H.-C.; Shen, S.-C., Eds.; Woodhead Publishing: Cambridge, U.K., 2013; pp 66−98.
(17) Maruska, H. P.; Tietjen, J. J. The Preparation and Properties of Vapor-Deposited Single-Crystal GaN. *Appl. Phys. Lett.* **1969**, *15*, 327−329.
(18) Kosicki, B. B.; Kahng, D. Preparation and Structural Properties of GaN Thin Films. *J. Vac. Sci. Technol.* **1969**, *6*, 593−595.
(19) Amano, H.; Sawaki, N.; Akasaki, I.; Toyoda, Y. Metalorganic Vapor-Phase Epitaxial-Growth of a High-Quality GaN Film Using an AlN Buffer Layer. *Appl. Phys. Lett.* **1986**, *48*, 353−355.
(20) Bernardini, F.; Fiorentini, V.; Vanderbilt, D. Spontaneous Polarization and Piezoelectric Constants of III-V Nitrides. *Phys. Rev. B: Condens. Matter Mater. Phys.* **1997**, *56*, R10024.
(21) Bernardini, F.; Fiorentini, V. Spontaneous versus Piezoelectric Polarization in III-V Nitrides: Conceptual Aspects and Practical Consequences. *Phys. Status Solidi B* **1999**, *216*, 391−398.
(22) Miller, D. A. B.; Chemla, D. S.; Damen, T. C.; Gossard, A. C.; Wiegmann, W.; Wood, T. H.; Burrus, C. A. Band-Edge Electroabsorption in Quantum Well Structures - The Quantum-Confined Stark-Effect. *Phys. Rev. Lett.* **1984**, *53*, 2173−2176.
(23) Ryou, J.-H.; Yoder, P. D.; Liu, J.; Lochner, Z.; Kim, H.; Choi, S.; Kim, H. J.; Dupuis, R. D. Control of Quantum-Confined Stark Effect in InGaN-Based Quantum Wells. *IEEE J. Sel. Top. Quantum Electron.* **2009**, *15*, 1080−1091.
(24) Takeuchi, T.; Sota, S.; Katsuragawa, M.; Komori, M.; Takeuchi, H.; Amano, H.; Akasaki, I. Quantum-Confined Stark Effect due to Piezoelectric Fields in GaInN Strained Quantum Wells. *Jpn. J. Appl. Phys.* **1997**, *36*, L382−L385.
(25) Im, J. S.; Kollmer, H.; Off, J.; Sohmer, A.; Scholz, F.; Hangleiter, A. Reduction of Oscillator Strength due to Piezoelectric Fields in GaN/$Al_xGa_{1-x}N$ Quantum Wells. *Phys. Rev. B: Condens. Matter Mater. Phys.* **1998**, *57*, R9435−R9438.
(26) Kim, M.-H.; Schubert, M. F.; Dai, Q.; Kim, J. K.; Schubert, E. F.; Piprek, J.; Park, Y. Origin of Efficiency Droop in GaN-Based Light-Emitting Diodes. *Appl. Phys. Lett.* **2007**, *91*, 183507.
(27) Waltereit, P.; Brandt, O.; Trampert, A.; Grahn, H. T.; Menniger, J.; Ramsteiner, M.; Reiche, M.; Ploog, K. H. Nitride Semiconductors Free of Electrostatic Fields for Efficient White Light-Emitting Diodes. *Nature* **2000**, *406*, 865−868.
(28) Liu, J. P.; Limb, J. B.; Ryou, J. H.; Yoo, D.; Horne, C. A.; Dupuis, R. D.; Wu, Z. H.; Fischer, A. M.; Ponce, F. A.; Hanser, A. D.; Liu, L.; Preble, E. A.; Evans, K. R. Blue Light Emitting Diodes Grown on Freestanding (11−20) *a*-Plane GaN Substrates. *Appl. Phys. Lett.* **2008**, *92*, 011123.
(29) Gardner, N. F.; Kim, J. C.; Wierer, J. J.; Shen, Y. C.; Krames, M. R. Polarization Anisotropy in the Electroluminescence of *m*-plane InGaN-GaN Multiple-Quantum-Well Light-Emitting Diodes. *Appl. Phys. Lett.* **2005**, *86*, 111101.
(30) Sharma, R.; Pattison, P. M.; Masui, H.; Farrell, R. M.; Baker, T. J.; Haskell, B. A.; Wu, F.; DenBaars, S. P.; Speck, J. S.; Nakamura, S. Demonstration of a Semipolar (10−1-3) InGaN/GaN Green Light Emitting Diode. *Appl. Phys. Lett.* **2005**, *87*, 231110.
(31) Park, S. H.; Chuang, S. L. Crystal-Orientation Effects on the Piezoelectric Field and Electronic Properties of Strained Wurtzite Semiconductors. *Phys. Rev. B: Condens. Matter Mater. Phys.* **1999**, *59*, 4725−4737.
(32) Kim, K.-C.; Schmidt, M. C.; Sato, H.; Wu, F.; Fellows, N.; Jia, Z.; Saito, M.; Nakamura, S.; DenBaars, S. P.; Speck, J. S. Study of Nonpolar m-Plane InGaN/GaN Multiquantum Well Light Emitting Diodes Grown by Homoepitaxial Metal-Organic Chemical Vapor Deposition. *Appl. Phys. Lett.* **2007**, *91*, 181120.
(33) Lin, Y.-D.; Chakraborty, A.; Brinkley, S.; Kuo, H. C.; Melo, T.; Fujito, K.; Speck, J. S.; DenBaars, S. P.; Nakamura, S. Characterization of Blue-Green *m*-Plane InGaN Light Emitting Diodes. *Appl. Phys. Lett.* **2009**, *94*, 261108.
(34) Aumer, M. E.; LeBoeuf, S. F.; Bedair, S. M.; Smith, M.; Lin, J. Y.; Jiang, H. X. Effects of Tensile and Compressive Strain on the Luminescence Properties of AlInGaN/InGaN Quantum Well Structures. *Appl. Phys. Lett.* **2000**, *77*, 821−823.
(35) Ryou, J. H.; Lee, W.; Limb, J.; Yoo, D.; Liu, J. P.; Dupuis, R. D.; Wu, Z. H.; Fischer, A. M.; Ponce, F. A. Control of Quantum-Confined Stark Effect in InGaN/GaN Multiple Quantum Well Active Region by p-Type Layer for III-Nitride-Based Visible Light Emitting Diodes. *Appl. Phys. Lett.* **2008**, *92*, 101113.
(36) www.str-soft.com/products/SimuLED.
(37) Hu, J.; Li, L.; Lin, H.; Zhang, P.; Zhou, W.; Ma, Z. Flexible Integrated Photonics: Where Materials, Mechanics and Optics Meet Invited. *Opt. Mater. Express* **2013**, *3*, 1313−1331.
(38) Ben Amar, A.; Faucher, M.; Brandli, V.; Cordier, Y.; Theron, D. Young's Modulus Extraction of Epitaxial Heterostructure AlGaN/GaN for MEMS Application. *Phys. Status Solidi A* **2014**, *211*, 1655−1659.
(39) Hastelloy C-276 is a Ni-based alloy with the composition of Ni 57.0 wt %, Mo 16.0 wt %, Cr 15.5 wt %, Fe 5.5 wt %, W 3.8 wt %.
(40) YSZ (yittria-stabilized zirconia) is a ZrO_2-based ceramic with 3 mol % Y_2O_3 added.
(41) Clickner, C. C.; Ekin, J. W.; Cheggour, N.; Thieme, C. L. H.; Qiao, Y.; Xie, Y. Y.; Goyal, A. Mechanical Properties of Pure Ni and Ni-Alloy Substrate Materials for Y-Ba-Cu-O Coated Superconductors. *Cryogenics* **2006**, *46*, 432−438.
(42) Adams, J. W.; Ruh, R.; Mazdiyasni, K. S. Young's Modulus, Flexural Strength, and Fracture of Yttria-Stabilized Zirconia versus Temperature. *J. Am. Ceram. Soc.* **1997**, *80*, 903−908.
(43) Dahiya, R. S.; Gennaro, S. Bendable Ultra-Thin Chips on Flexible Foils. *IEEE Sens. J.* **2013**, *13*, 4030−4037.
(44) Lee, S.; Kwon, J.-Y.; Yoon, D.; Cho, H.; You, J.; Kang, Y. T.; Choi, D.; Hwang, W. Bendability Optimization of Flexible Optical Nanoelectronics via Neutral Axis Engineering. *Nanoscale Res. Lett.* **2012**, *7*, 256.
(45) Li, H. Y.; Guo, L. H.; Loh, W. Y.; Bera, L. K.; Zhang, Q. X.; Hwang, N.; Liao, E. B.; Teoh, K. W.; Chua, H. A.; Shen, Z. X.; Cheng, C. K.; Lo, G. Q.; Balasubramanian, N.; Kwong, D. L. Bendability of Single-Crystal Si MOSFETs Investigated on Flexible Substrate. *IEEE Electron Device Lett.* **2006**, *27*, 538−541.
(46) Petti, L.; Muenzenrieder, N.; Salvatore, G. A.; Zysset, C.; Kinkeldei, T.; Buethe, L.; Troester, G. Influence of Mechanical Bending on Flexible InGaZnO-Based Ferroelectric Memory TFTs. *IEEE Trans. Electron Devices* **2014**, *61*, 1085−1092.
(47) Gotz, W.; Johnson, N. M.; Walker, J.; Bour, D. P.; Street, R. A. Activation of Acceptors in Mg-Doped GaN Grown by Metalorganic Chemical Vapor Deposition. *Appl. Phys. Lett.* **1996**, *68*, 667−669.
(48) Mnatsakanov, T. T.; Levinshtein, M. E.; Pomortseva, L. I.; Yurkov, S. N.; Simin, G. S.; Khan, M. A. Carrier Mobility Model for GaN. *Solid-State Electron.* **2003**, *47*, 111−115.
(49) Khokhlev, O. V.; Bulashevich, K. A.; Karpov, S. Y. Polarization Doping for III-Nitride Optoelectronics. *Phys. Status Solidi A* **2013**, *210*, 1369−1376.
(50) Li, S. B.; Ware, M. E.; Kunets, V. P.; Hawkridge, M.; Minor, P.; Wu, J.; Salamo, G. J. Polarization Induced Doping in Graded AlGaN Films. *Phys. Stat. Sol. (c)* **2011**, *8*, 2182−2184.
(51) A Term, band "bending" is commonly used in semiconductor communities; however, the term band "tilt" is used in this study to avoid confusion with III-N physical structure bending by external loads to apply external strain.
(52) Perlin, P.; Kisielowski, C.; Iota, V.; Weinstein, B. A.; Mattos, L.; Shapiro, N. A.; Kruger, J.; Weber, E. R.; Yang, J. W. InGaN/GaN Quantum Wells Studied by High Pressure, Variable Temperature, and Excitation Power Spectroscopy. *Appl. Phys. Lett.* **1998**, *73*, 2778−2780.
(53) Choi, S.; Kim, H. J.; Kim, S.-S.; Liu, J.; Kim, J.; Ryou, J.-H.; Dupuis, R. D.; Fischer, A. M.; Ponce, F. A. Improvement of Peak Quantum Efficiency and Efficiency Droop in III-Nitride Visible Light-Emitting Diodes with an InAlN Electron-Blocking Layer. *Appl. Phys. Lett.* **2010**, *96*, 243506.
(54) Schubert, E. F.; Kim, J. K. Solid-State Light Sources Getting Smart. *Science* **2005**, *308*, 1274−1278.

DOI: 10.1021/acsphotonics.5b00745
ACS Photonics 2016, 3, 486−493